Experimental and Numerical Investigation of Fluid Dynamics of a Bounded Equilateral Triangular Jet

R.RIAHI[1], F.BAGHERI[1], B.FARHANIEH[2] and A.HAJILOUY[3]
Department of Mechanical Engineering
Sharif University of Technology
Azadi Av., P. O. Box 11365-9567-Tehran
IRAN

Abstract: - In the present study, the fluid characteristics of a triangular turbulent jet flow are considered experimentally and numerically. The results of spatially developed three dimensional jet, issued from an equilateral triangular nozzle are presented. The jet is discharged to a bounded domain. The hot-wire anemometry is used for experimental study. A numerical method employing control volume approach with collocated grid arrangement which couples the velocity and pressure fields with SIMPLEC algorithm is introduced to discrete the governing equations of fluid flow. The turbulent stresses are approximated using k-ε model. The velocity field is presented using profiles and contours. Comparison of numerical and experimental results shows a good agreement.

Key-Words: - Triangular jet, Bounded domain, Hot-wire anemometry, Numerical simulation, Velocity profiles, Turbulence Intensity

1 Introduction

Jet flows represent a very good benchmark for research into the physics of turbulent fluid flow. They are also of great interests for many engineering applications such as internal combustion engines, propulsions, spray driers, laser machining of metals, mixing of chemical reactants, cooling of blades, etc. While there are considerable numbers of numerical and experimental investigations on planar, circular, rectangular and elliptic jets [1-10], there are only few works reported on the studies of triangular jet in the open literature. R.S Miller, C.K Madnia [1] studied numerically, using direct numerical simulation, a few non circular cross section jets. They investigated the fluid dynamics of the flow field and combustion of a variety of non-circular jets at a low specified Re number. The jets were discharged to a non-stagnant ambient. The influence of jet cross section on the flow and the combustion were studied. They showed that the triangular jets have higher mixing ability in comparison to other non-circular jets. Quinn [2] has experimentally studied a triangular cross section free jet at a high Re number, using Hot-Wire anemometry. He measured velocity variation of the jet and presented the contours of average and fluctuating velocity components.

1. Graduate students
2. Professor
3. Associate Professor

In the present work, an equilateral triangular bounded jet, discharging steadily from a slot to stagnant bounded domain at different Reynolds numbers is considered. The fluid dynamics of the velocity field is studied using contours and profiles. Also the centerline velocity decay is presented.

2 Problem Formulation

2.1 Physics of Interest

The geometry of interest is shown in Fig.1. The air is discharged from an equilateral triangular slot into a bounded air domain. A symmetry surface divides the domain into two identical parts. Advantage of this feature is limiting calculation domain to only half the nozzle. The fluid characteristics of turbulent and incompressible flow along the jet are to be determined.

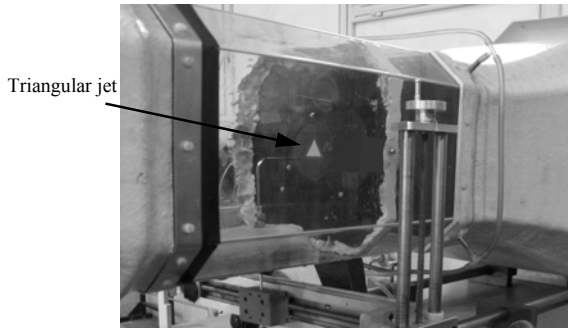

Fig.1 The geometry under consideration

2.2 Experimental arrangement and procedure

The flow facility is of the suction type and consists of subsonic wind tunnel with a small axial flow fan and sharp edged equilateral triangular slot.

The Plexy glass plate is machined to outsource an equilateral triangular slot in its center which is schematically shown in Fig.2.

Air enters the test section through a well-designed contraction entrance of which an aluminum honeycomb with hexagonal cell is placed to ensure the flow steadiness in both magnitude and direction resulting in flat transverse velocity profiles. A low angle diffuser at the outlet end contributes to flow stability in the parallel octagonal test section where the octagonal Plexy glass plate with equilateral triangular slot is installed.

The jet issues from the slot into the diffuser and the five-blade fan located in the downstream of the diffuser draws the air to the outlet. The fan is driven by an AC motor controlled by an inverter speed control unit.

The sensing probe is moved in the flow field by a manual 3-D traversing system of leading screw type with 0.25mm positioning accuracy in three directions.

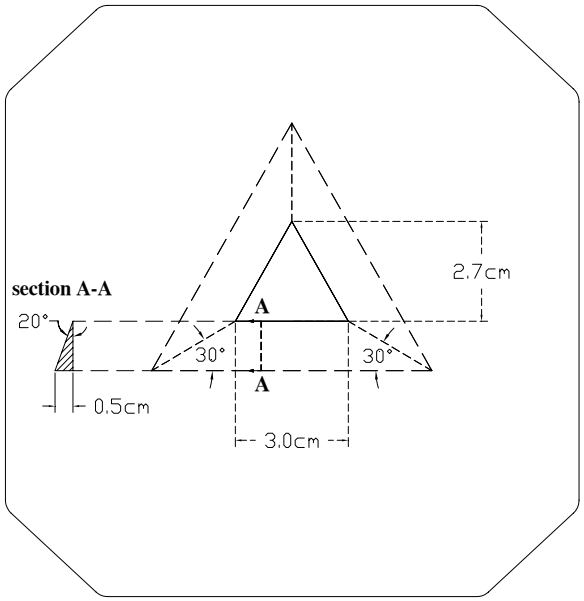

Fig.2 Equilateral triangular slot dimensions

A definition sketch of the coordinate system and the corresponding component of the mean velocity vector in the streamwise (x) direction are presented in Fig.3.

Straight miniature hot-wire probes are used for the mean velocity and turbulence measurements. The hot-wire probe is operated by linearized constant temperature anemometers (CTA) using a resistance ratio of 1.8.

The aforementioned probe is calibrated in the test section of the wind tunnel using Pitot static tube.
A 12-bit A/D conversion board specified with up to 100kHz sampling rate and 16 analog input channel along with multiplexer board is employed to digitize the hot-wire signals.

Signal conditioning is affected by either low pass analog filters with a 5 kHz cut-off frequency, 40dB/decade roll-off or an amplifier. The mean profile and RMS fluctuating velocities are obtained with Lab View software with sampling rate of 15 kHz in 9 even points (5mm each) along with the triangle's height and at different downstream stations of the nozzle exit.

2.3 Governing Equations

The governing equations are the continuity and momentum equations. The flow is studied with the following assumptions: steady state, constant fluid properties and negligible viscous dissipation.
The governing equations read:

$$\frac{\partial \rho}{\partial t} + \frac{\partial}{\partial x_j}(\rho U_j) = 0 \qquad (1)$$

$$\frac{\partial}{\partial x_j}\left(\rho U_i U_j\right) = -\frac{\partial P}{\partial x_i} + \frac{\partial}{\partial x_j}\left(\mu \frac{\partial U_i}{\partial x_j}\right) - \frac{\partial}{\partial x_j}\left(\rho \overline{u_i u_j}\right) \qquad (2)$$

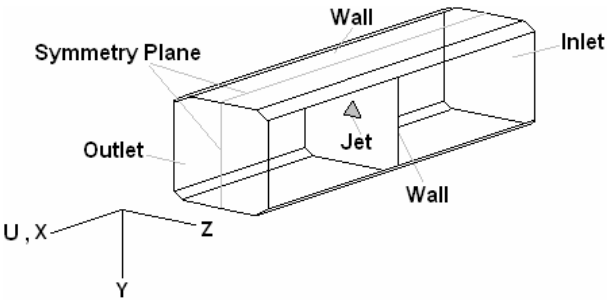

Fig.3 Schematic of the geometry under consideration

A closure of the equation (2) by means of the turbulence model results in the additional equations

for the turbulent kinetic energy and its dissipation rate:

$$\rho\overline{u_i u_j} = -\mu_t\left(\frac{\partial U_i}{\partial x_j}+\frac{\partial U_j}{\partial x_i}\right)+\frac{2}{3}\rho k\delta_{ij} \quad (3)$$

Where the turbulent eddy viscosity is defined as:

$$\mu_t - C_\mu \rho \frac{k^2}{\varepsilon} \quad (4)$$

The conservation equations for turbulent kinetic energy and its dissipation rate are:

$$\frac{\partial}{\partial x_j}\left(\rho U_j k\right)=\frac{\partial}{\partial x_j}\left(\frac{\mu_t}{\sigma_k}\frac{\partial k}{\partial x_j}\right)+G-\rho\varepsilon \quad (5)$$

$$\frac{\partial}{\partial x_j}\left(\rho U_j \varepsilon\right)=\frac{\partial}{\partial x_j}\left(\frac{\mu_t}{\sigma_\varepsilon}\frac{\partial \varepsilon}{\partial x_j}\right)+c_1\frac{\varepsilon}{k}G-c_2\rho\frac{\varepsilon^2}{k} \quad (6)$$

The rate of turbulent kinetic energy production is obtained by:

$$G=\mu_t\left(\frac{\partial U_j}{\partial x_i}+\frac{\partial U_i}{\partial x_j}\right)\frac{\partial U_i}{\partial x_j} \quad (7)$$

The values of the constants appearing in the k-ε equation are given in Table 1.

Table 1- Turbulence model constants [11]

Constant	c_1	c_2	c_μ	σ_k	σ_ε
Value	1.44	1.92	0.09	1.0	1.3

3 Numerical Simulation

A finite volume method with collocated variable arrangement is used for solving the equation system [12]. The pressure and mean velocity fields are coupled by the SIMPLEC algorithm. M. Peric and R. Kessler interpolation technique [13] is used to prevent pressure field oscillations. The dissipative terms are discretized with the central differencing scheme. Van Leer [14] second order difference scheme is adopted for the convective terms in the momentum and energy equations. The discretized equations are solved iteratively using the tridiagonal matrix algorithm line solver. The convergence criterion is that the sum of the absolute residuals divided by the inlet fluxes is below 10-5 for all variables. Due to the existence of strong velocity gradients around the jet centerline, a non-uniform mesh of 140×100×100 is adopted for discretizing the flow domain (see Fig.4). The Grid independency condition is studied with 120×90×90 & 100×80×80 nodes. The error between finer meshes was less than 10-5. The comparative results for the velocity profiles are presented at Fig.5.

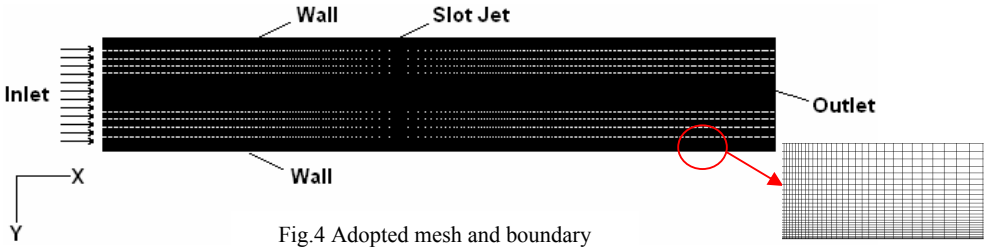

Fig.4 Adopted mesh and boundary

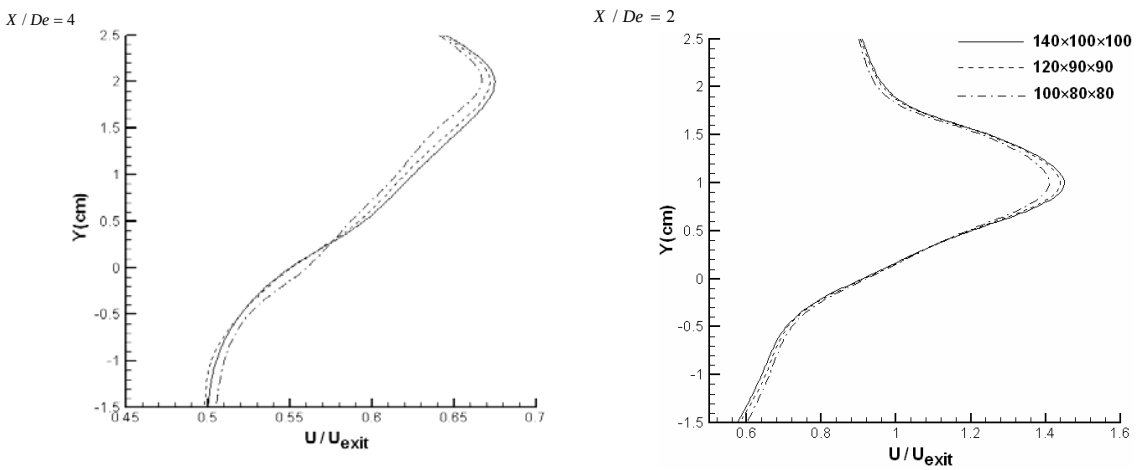

Fig.5 grid independency check with velocity profile

4 Results and Discussion

The velocity vectors and the contours for the flow field are obtained and presented at different planes. The velocity contours at symmetry plane are presented in Figs.6. The contours of the velocity field indicate how the jet spreads due to the strong shear layer effects. The change in direction of flow near the edge of jet is representative of intense gradient in that location, which is the reason for jet spread at the domain. The cross flow vectors at different downstream locations are shown in Fig.7 and The start point of X axis is the solid plate.

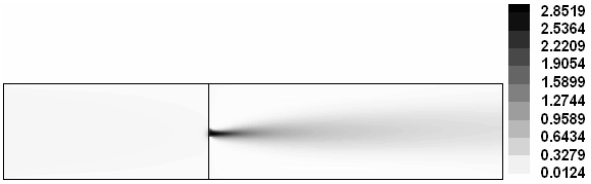

Fig.6 Velocity Contours (m/s) at symmetry plane

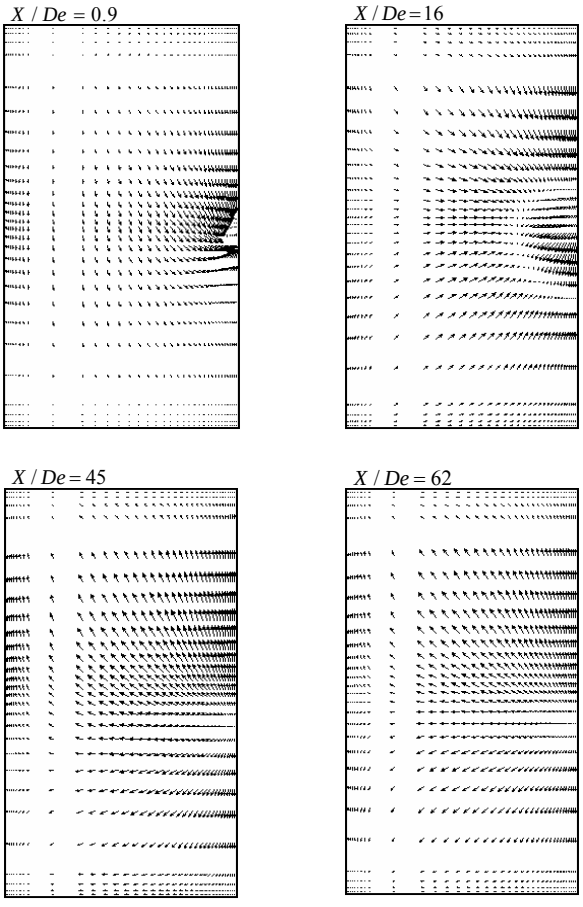

Fig.7 Cross stream flow field at some X/D_e

4.1 Mean Velocity Comparison

The centerline normalized velocity decay curve along the flow for experimental and numerical investigation is plotted in Fig.8. It can be seen from this figure that close to the nozzle, an overshoot has takes place. This is the result of curvature of flow pattern to the jet centerline at the discharge location which causes the increment of velocity in that area.

The velocity profiles at symmetry plane for different Reynolds numbers are shown in Figs.9-10. The profiles become smoother further away from the discharge location and good agreement between the experimental and the numerical results could be observed in these figures.

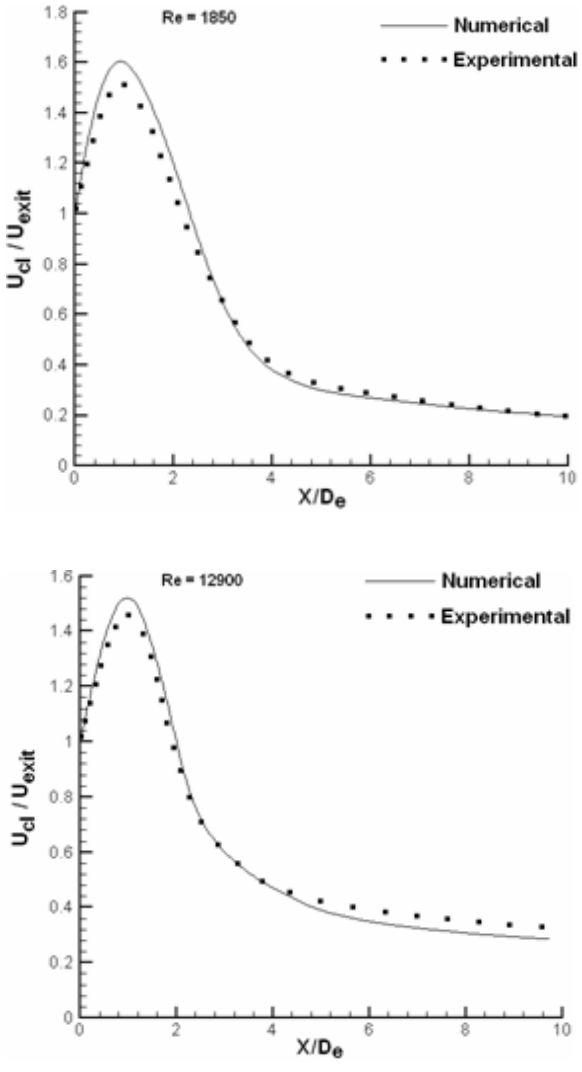

Fig.8 Centerline normalized velocity variations for two different Re

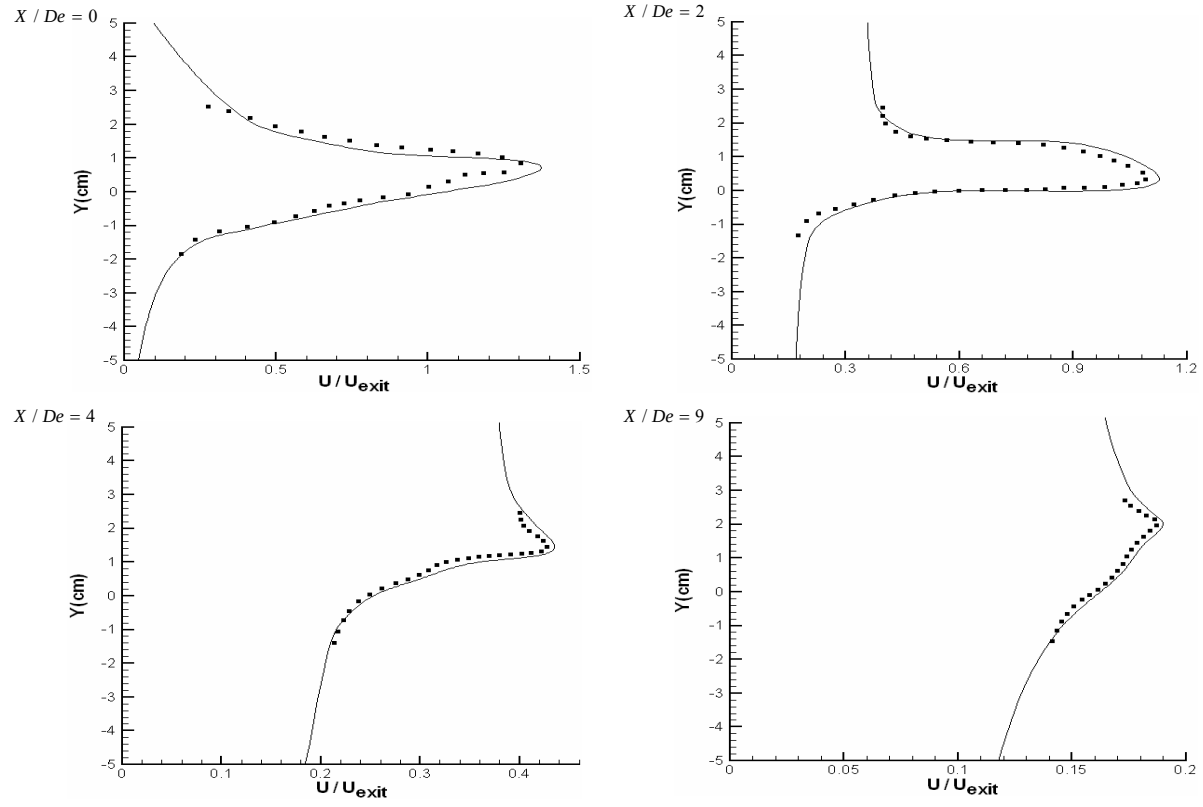

Fig.9 Normalized velocity profiles at Re=1850

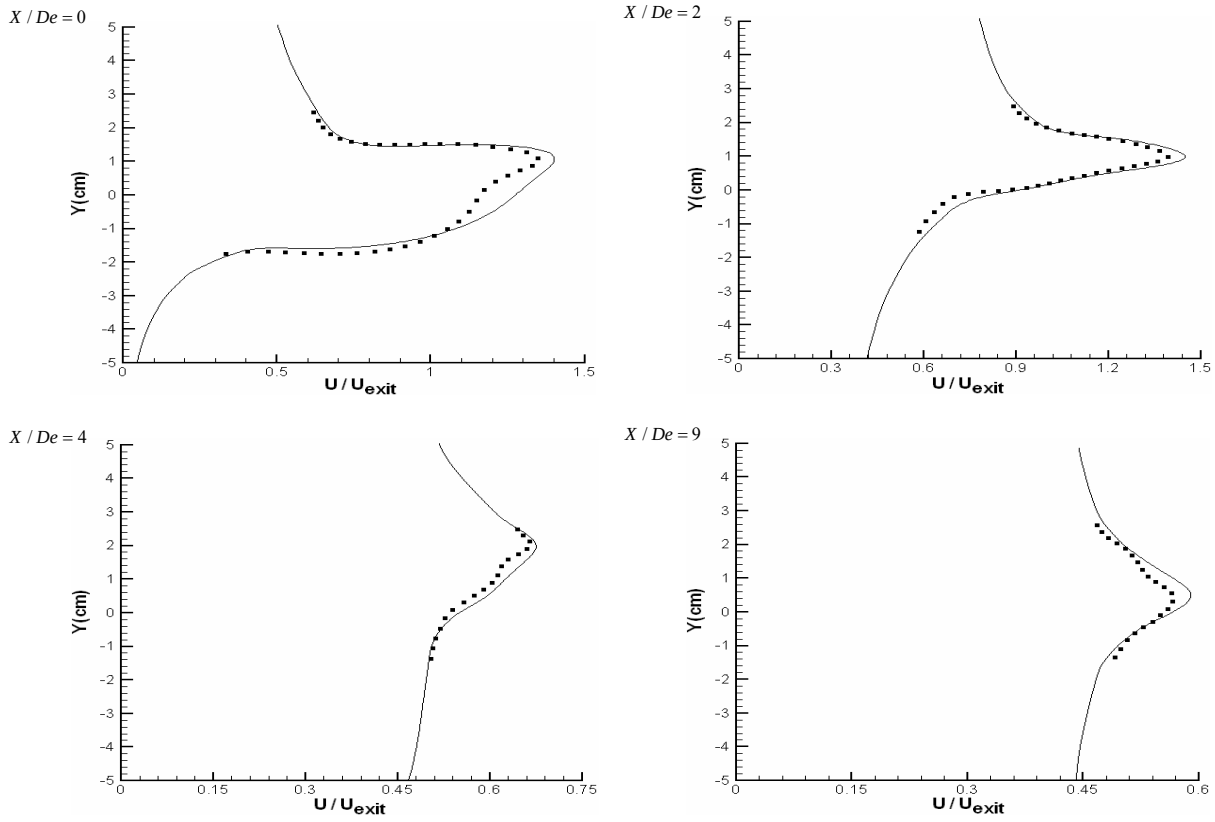

Fig.10 Normalized velocity profiles at Re=12900

4.2 Turbulence Intensity

The streamwise turbulence intensity variation along the jet centerline is plotted in Fig.11 at five different Reynolds numbers. It's observed that in the flow initial zone the slope of the streamwise turbulence intensity is increased. This increase is a consequence of shear layer growth and the resulting high production of turbulence which is then diffused to the jet centerline. Furthermore, large streamwise turbulence intensity is found by decreasing the Reynolds number in high X/De region. The decrease in the streamwise turbulence intensity in the region X/De= 2.5 to 4.0, originates through the merging of the three shear layers of the aforementioned equilateral triangle slot.

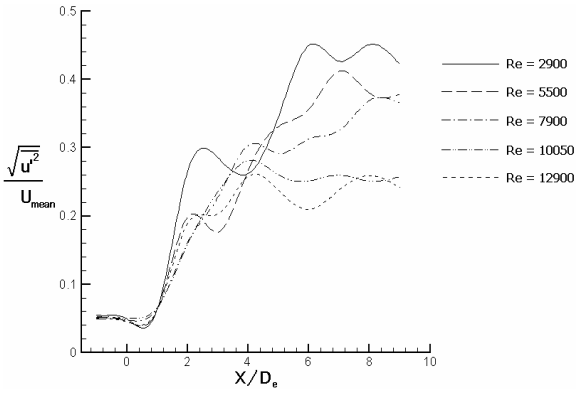

Fig.11 Streamwise turbulence intensity

5 Conclusion

The fluid characteristics of a developing bounded jet emanating from an equilateral triangular nozzle are investigated experimentally and numerically. For the experimental study the hot-wire anemometry and for the numerical simulation a finite-volume method with collocated grid arrangement using k-ε turbulent model were employed. The jet centerline velocity decay shows that the jet spreads in the bounded domain and reaches the domain bounds.

The velocity profiles were obtained at different cross section along the jet path for two different Reynolds numbers. The results show a small upward deviation of the jet from the centerline.

References:

[1] R.S. Miller, C.K. Madnia and P. Givi, Numerical Simulation of Non-Circular Jets, *Journal of Computers and Fluids*, 1995, pp. 1-25.

[2] W.R. Quinn, Mean Flow and Turbulence Measurements in a Triangular Turbulent Free Jet, *International Journal of Heat and Fluid Flow*, 1990, pp. 20-25.

[3] - A.A Mostafa, M.M.Khalifa, E.A.Shabana, 2000. Experimental and numerical investigation of multiple rectangular jets, Experimental thermal and fluid sciences 171-178

[4] X. Zhou, Z. Sun, F. Durst, G. Brenner, Numerical Simulation of Turbulent Jet Flow and Combustion, *International Journal of Computers and Mathematics with Applications*, 1999, pp. 179-191.

[5] B. Rembold, N.A. Adams, L. Kleiser, Direct Numerical Simulation of a Transitional Rectangular Jet, *International Journal of Heat and Fluid Flow*, 2002, pp. 547-553.

[6] Ch. Fureby, F.F. Grinstein, Large Eddy Simulation of High Reynolds Number Free and Wall-Bounded Flows, *Journal of Computational Physics*, 2002, pp. 68-97.

[7] J. J. Mc Guirk, W. Rodi, The Calculation of Three-Dimensional Turbulent Free Jets, *Turbulent shear flows first conference*, Pennsylvania, 1977, pp. 71-83.

[8] C. Cornaro, A.S. Fleischer, R.J. Goldstein, Flow Visualization of a Round Jet Impinging on Cylindrical Surfaces, *Journal of Experimental Thermal and Fluid Science*, 1999, pp. 66-78.

[9] K. Knowles, M. Myszko, Turbulence Measurements in Radial Wall-Jets, *Journal of Experimental Thermal and Fluid Science*, 1998, pp. 71-78.

[10] H.A. Warda, S.Z. Kassab, K.A. Elshorbagy, E.A. Elsaadawy, An Experimental Investigation of the Near-Field Region of Free Turbulent Round Central and Annular Jets, *Journal of Flow Measurement and Instrumentation*, 1999, pp1-14.

[11] Chen. Ch, Jaw. S, Fundamentals of Turbulence Modeling, Taylor and Francis Company, New York, 1997.

[12] B. Farhanieh, L. Davidson, B. Sunden, Employment of Second-Moment Closure for Calculation of Turbulent Recalculating Flows in Complex Geometries with Collocated Variable Arrangement, *International Journal of Numerical Methods in Fluids*, Vol. 16, 1993, pp 525-544.

[13] M. Peric, R. Kessler, G. Scheuerer, Comparison of Finite-Volume Numerical Methods with Staggered and Collocated Grids, *Journal of Computers and Fluids*, Vol. 16, 1988, pp. 389-403.

[14] B. Van Leer, Towards the Ultimate Conservative-Difference-Scheme, Conservation Combined in a Second Order Scheme, *Journal of Computational Physics*, Vol. 14, 1974, pp. 361-370.